Cellular Physiology and Biochemistry

Cell Physiol Biochem 2015;35:148-159
DOI: 10.1159/000369683
Published online: January 02, 2015
Accepted: November 05, 2014

Karger Open access

1421-9778/15/0351-0148$39.50/0

Original Paper

Influence of *N*-Acetylcysteine on Oxidative Stress in Slow-Twitch Soleus Muscle of Heart Failure Rats

Paula F. Martinez[a,b] Camila Bonomo[a] Daniele M. Guizoni[a]
Silvio A. Oliveira Junior[a,b] Ricardo L. Damatto[a] Marcelo D.M. Cezar[a]
Aline R.R. Lima[a] Luana U. Pagan[a] Fabio R. Seiva[c] Denise C. Fernandes[d]
Francisco R.M. Laurindo[d] Ethel L.B. Novelli[a] Luiz S. Matsubara[a]
Leonardo A.M. Zornoff[a] Katashi Okoshi[a] Marina P. Okoshi[a]

[a]Botucatu Medical School, UNESP, Botucatu, [b]Federal University of Mato Grosso do Sul, Campo Grande, [c]North of Parana State University, Bandeirantes, [d]Heart Institute (InCor)-HC-FMUSP, Vascular Biology Laboratory, Sao Paulo, Brazil

Key Words
Heart failure • Skeletal muscle • NADPH oxidase • Myocardial infarction • *N*-acetylcysteine • Reactive oxygen species

Abstract
Background: Chronic heart failure is characterized by decreased exercise capacity with early exacerbation of fatigue and dyspnea. Intrinsic skeletal muscle abnormalities can play a role in exercise intolerance. Causal or contributing factors responsible for muscle alterations have not been completely defined. This study evaluated skeletal muscle oxidative stress and NADPH oxidase activity in rats with myocardial infarction (MI) induced heart failure. ***Methods and Results:*** Four months after MI, rats were assigned to Sham, MI-C (without treatment), and MI-NAC (treated with *N*-acetylcysteine) groups. Two months later, echocardiogram showed left ventricular dysfunction in MI-C; NAC attenuated diastolic dysfunction. In soleus muscle, glutathione peroxidase and superoxide dismutase activity was decreased in MI-C and unchanged by NAC. 3-nitrotyrosine was similar in MI-C and Sham, and lower in MI-NAC than MI-C. Total reactive oxygen species (ROS) production was assessed by HPLC analysis of dihydroethidium (DHE) oxidation fluorescent products. The 2-hydroxyethidium (EOH)/DHE ratio did not differ between Sham and MI-C and was higher in MI-NAC. The ethidium/DHE ratio was higher in MI-C than Sham and unchanged by NAC. NADPH oxidase activity was similar in Sham and MI-C and lower in MI-NAC. Gene expression of $p47^{phox}$ was lower in MI-C than Sham. NAC decreased NOX4 and $p22^{phox}$ expression. ***Conclusions:*** We corroborate the case that oxidative stress is increased in skeletal muscle of heart failure rats and show for the first time that oxidative stress is not related to increased NADPH oxidase activity.

E.L.B. Novelli-in memoriam

Marina Politi Okoshi

Departamento Clínica Medica, Faculdade Medicina Botucatu/UNESP
Rubiao Junior, S/N, CEP-18618-970, Botucatu, SP, (Brazil)
Tel. +55 14 3880 1171, Fax +55 14 3882 2238. E-Mail mpoliti@fmb.unesp.br

Introduction

Chronic heart failure is characterized by decreased exercise capacity with early exacerbation of symptoms, such as fatigue and dyspnea. Intrinsic skeletal muscle abnormalities have been described in heart failure patients and hypothesized to play a role in exercise intolerance [1-7]. Skeletal muscle alterations such as atrophy, fibrosis, decreased oxidative capacity, altered myosin distribution, and contractile dysfunction have been well characterized in several experimental and clinical heart failure studies [3, 6-11]. However, the causal or contributing factors responsible for muscle alterations have not been completely defined.

There is substantial evidence that systemic and myocardial oxidative stress is augmented during heart failure [12, 13]. More recently, increased oxidative stress was also observed in skeletal muscle [14-16]. Mice with myocardial infarction presented increased lipoperoxidation and reactive oxygen species (ROS) generation, with no changes in antioxidant enzymes activity [15]. In vastus lateralis muscle biopsies of patients with heart failure, Linke at al. [14] observed increased nitrotyrosine concentration and lipoperoxidation associated with reduced antioxidant enzymes gene expression and activity. However, sources of ROS have not been completely defined.

NADPH oxidase (NOX) family is composed of enzymes whose main function is ROS production [17]. For a long time, only phagocytes were considered to produce superoxide by NADPH oxidase activity. However, in the last decade, six homologues of phagocyte NOX2 ($gp91^{phox}$) subunit were described and identified in various tissues [17]. NOX2 and NOX4 are the two NADPH oxidase isoforms expressed in skeletal muscle [18, 19]. These enzymes share the capacity to generate superoxide and other ROS [17]. Although NOX isoforms present similarities, they differ in mode of interaction with the transmembrane protein $p22^{phox}$, and the requirement for additional activation factors. In heart failure, Ohta et al. [20] detected increased NADPH oxidase activity in skeletal muscle of infarcted mice; however, they did not evaluate gene expression of NADPH oxidase subunits or H_2O_2 generation.

To demonstrate the role of oxidative stress in heart failure-associated skeletal muscle alterations it is important to perform functional interference with an antioxidant. Glutathione (L-γ glutamyl-cysteinyl-glycine) is an endogenous tripeptide that plays a fundamental role in cellular defense against oxidative stress [21, 22]. During heart failure, glutathione redox status is altered and its total concentration decreased in cardiac tissue [23]. *N*-acetylcysteine (NAC) is a molecule with antioxidant properties; it contains a sulfhydryl group and is a source of cysteine to glutathione synthesis. In a recent study, administration of NAC restored total glutathione levels and reduced oxidative stress markers in infarcted rat heart [23].

In this study we validated the case that oxidative stress is increased in skeletal muscle of HF rats and showed that oxidative stress is not related to increased NADPH oxidase activity.

Material and Methods

Ethics Statement

This study was carried out in strict accordance with the recommendations in the Guide for the Care and Use of Laboratory Animals of the National Institutes of Health. The protocol was approved by the Committee on the Ethics of Animal Experiments of Botucatu Medical School, Universidade Estadual Paulista, UNESP (Protocol Number: 707). All surgery was performed under anesthesia, and all efforts were made to minimize suffering.

Experimental groups

Male Wistar rats (200–250 g) were housed in a room under controlled temperature and light-dark cycle. Food and water were supplied *ad libitum*. All experiments were approved by the Ethics Committee of Botucatu Medical School, Universidade Estadual Paulista, UNESP.

Myocardial infarction (MI) was induced by ligating the anterior descending coronary artery [24]. Four months later, rats were assigned to three groups: Sham, MI-C (MI without treatment), and MI-NAC (MI treated with *N*-acetylcysteine, 120 mg/kg/day). Six months after surgery, rats were euthanized. At euthanasia, two observers determined whether the clinical and pathologic heart failure features were present or absent. Tachypnea/labored respiration was the clinical finding. Pathologic findings included pleuropericardial effusion, left atrial thrombi, pulmonary congestion (lung weight-to-body weight (BW) ratio >2 standard deviation above sham group mean), and right ventricular hypertrophy (right ventricle weight-to-BW ratio >0.8 mg/g) [24, 25].

Echocardiographic evaluation

Echocardiogram was performed before and after NAC treatment (Vivid S6, General Electric Medical Systems, Tirat Carmel, Israel) using a 5 to 11.5 MHz electronic transducer, according to a previously described method [26-29].

Infarct size

Left ventricle samples were fixed in a 10% buffered formalin solution for 48 h and stained with picrosirius red according to the previously described method [24, 30]. The lengths of the infarcted and viable myocardial for both the endocardial and epicardial circumferences were determined by planimetry. Infarction size was calculated by dividing the sum of endocardial and epicardial infarcted ventricular lengths by the sum of total (infarcted and viable myocardial) endocardial and epicardial ventricular circumferences. The measurements were acquired from midventricular slices (5-6 mm from the apex), under the assumption that the left midventricular slice shows a close linear relation with the sum of the measurements from all heart slices. A compound microscope (Leica DM LS; Nussloch, Germany) attached to a computerized imaging analysis system (Media Cybernetics, Silver Spring, MD, USA) was used to perform the measurements. Rats with small MI size (<30%) were excluded.

Antioxidant enzymes activity and lipid hydroperoxide concentration

Soleus muscle samples (~200 mg) were homogenized in 5 mL of a cold 0.1 M phosphate buffer, pH 7.0. Tissue homogenates were prepared in a motor-driven Teflon-glass Potter-Elvehjem, tissue homogeniser. The homogenate was centrifuged at 10,000 g, for 15 min, 4 °C, and the supernatant was assayed for total protein, lipid hydroperoxide (LOOH), and glutathione peroxidase (GSH-Px, E.C.1.11.1.9), catalase (E.C.1.11.1.6.), and superoxide dismutase (SOD, E.C.1.15.1.1.) activities by spectrophometry [31]. Enzyme activities were analyzed at 25 °C using a microplate reader (μQuant-MQX 200 with Kcjunior software to computer system control, Bio-Tec Instruments, Winooski, Vermont, USA). Spectrophotometric determinations were performed in a Pharmacia Biotech spectrophotometer with temperature-controlled cuvette chamber (UV/visible Ultrospec 5000 with Swift II applications software to computer system control, 974213, Cambridge, England, UK). All reagents were purchased from Sigma-Aldrich (St. Louis, MO, USA).

Glutathione peroxidase was assayed using 0.15 M phosphate buffer (pH 7.0), containing 5 mM EDTA, 0.0084 M NADPH, 4 μg of GSSG-reductase, 1.125 M NaN3 (sodium aside) and 0.15 M GSH in a total volume of 0.3 ml [32]. To assess superoxide dismutase activity (SOD, E.C. 1.15.1.1), we performed a microplate assay based superoxide mediated-nitro blue tetrazolium (NBT) reduction by an aerobic mixture of NADH (reduced nicotinamide adenine dinucleotide) and phenazine methosulfate (PMS). The complete reaction system consisted of 50 mM phosphate buffer (pH 7.4), 0.1 mM EDTA, 50 μM NBT, 78 μM NADH and 3.3 μM PMS [33]. Catalase activity was determined with phosphate buffer (pH 7.0). The assay mixture consisted of 0.019 M hydrogen peroxide and buffer solution in a final volume of 0.3 ml [34].

Lipid hydroperoxide was measured through hydroperoxide-mediated oxidation of Fe^{2+}, with 100 μl of sample and 900 μl of a reaction mixture containing 250 μM FeSO4, 25 mM H2SO4, 100 μM xylenol orange and 4 mM butylated hydroxytoluene (BHT) in 90% (v/v) methanol [35].

Malondialdehyde serum concentration

Lipid peroxidation was assessed by measuring malondialdehyde (MDA) by high performance liquid chromatography (HPLC), as reported previously [36]. Briefly, 100 μL of serum was treated with butylated hydroxytoluene (BHT 5% in EtOH), followed by protein precipitation using trichloroacetic acid (TCA 10% w/v), at 95°C for 20 min. The sample was cooled in ice and centrifuged for 5 min at 12,000 g. Supernatant

(300 µL) was reacted with 650 µL of thiobarbituric acid (TBA 0.4% w/v, in acetate buffer, pH 3.5) and 50 µL of 3,065 M KOH, warmed to 95 °C for 45 min, and cooled on ice for 5 min. Then, the sample was analyzed for MDA-TBA adducts by an HPLC system with a Pecosphere-3 C18 column (83 × 4.6 mm) using a fluorescence detector (Waters 2475), which was set Ex 515 nm and Em 553 nm. The HPLC mobile phase was 20 mM potassium phosphate buffer:acetonitril (80:20, v:v), and the flow rate was set at 0.8 mL/min. The lower limit of detection is 0.2 pmol for the MDA-TBA adduct. MDA was quantified by comparison of integrated peak areas between samples and standard solution under identical chromatographic conditions.

3-Nitrotyrosine concentration measurement

Nitrotyrosine concentration was measured in soleus muscle by enzyme-linked immunosorbent assay (ELISA) using *OxiSelect™ Nitrotyrosine ELISA Kit* (STA-305, Cell Biolabs, San Diego, CA, USA).

ROS generation

Muscle fragment (~100 mg) was washed in PBS and incubated in a solution containing PBS/DTPA and 150 µM DHE for 25 min at 37 °C in a dark room. Then, muscle fragment was washed in PBS, transferred to liquid nitrogen, and homogenised with mortar and pestle. The homogenate was resuspended in acetonitrile (0.5 ml), sonicated (3 cycles at 8 W for 10 s), and centrifuged (12,000 g for 10 min at 4°C). Supernatant was dried under vacuum (Speed Vac Plus model SC-110A, Thermo Savant) and pellets maintained at -20°C in the dark until analysis. Samples were resuspended in 80 µL deionized water and injected into HPLC system. Total ROS generation was evaluated in soleus muscle by quantification of two dihydroethidium (DHE) oxidation-derived fluorescent compounds, 2-hydroxyethidium (EOH) and ethidium, using HPLC according to a previously described method [37, 38]. EOH is generated when DHE is oxidized by anion superoxide, while ethidium production is associated to heme proteins levels and peroxidase activity. DHE-derived products were expressed as ratios of generated EOH and ethidium over consumed DHE (initial DHE concentration minus remaining DHE).

NADPH oxidase activity

NADPH oxidase activity was evaluated in membrane-enriched cellular fraction by quantifying DHE oxidation-derived fluorescent compounds, EOH and ethidium by HPLC according to a previously described method [37, 38].

Soleus muscle was carefully washed in PBS to remove blood. Muscle fragments (~200 mg) were homogenized in 1 mL of ice-cold lysis buffer containing 50 mM Tris (pH 7.4), 100 mM DTPA, 0,1% β-mercaptoethanol, and protease inhibitors. Then, the samples were sonicated (3 cycles of 10 s at 8 Watts) and centrifuged at 1,000 g for 3 min, at 4 °C. The supernatant was transferred to another microtube and centrifuged at 18,000 g for 10 min, at 4 °C. After, the supernatant was transferred to ultracentrifuge tubes and centrifuged at 100.000 g for 45 min, at 4 °C. The supernatant was then discarded and the precipitate (pellet) was resuspended in 100 µL of lysis buffer [38]. Total protein content was quantified by the Bradford method.

Subsequently, 20 µg of membrane-enriched cellular fraction were incubated in phosphate buffer (50 mM, pH 7.4, with 0.1 mM DTPA) containing DHE (50 µM) and NADPH (300 µM), to a final volume of 100 µL, for 30 min, at 37 °C, in the dark. After 40 µL of 10% trichloroacetic acid were added, the samples were ice-cooled for 10 min at the dark, and centrifuged at 12,000 g for 10 min, at 4 °C. The supernatant was analyzed by HPLC and the fluorescent DHE-derived products were quantified, according to a previously described method [37, 38].

Membrane-enriched cellular fraction was also submitted to microplate assay with Amplex Red® (Invitrogen, Carlsbad, CA, EUA). In this analysis, NADPH oxidase activity was determined by H_2O_2 accumulation. Sample of membrane-enriched cellular fraction (20 µg) was incubated with 250 µM NADPH in phosphate buffer solution (50 mM, pH 7.4, with 0.1 mM DTPA) in presence of HRP (horseradish peroxidase, 0.2 U/µL) and Amplex Red® reagent (140 µM), at 37 °C, in the dark (final volume: 120 µL). Absorbance was measured at 575 nm for 60 min in a spectrofluorometer (Spectramax 340, Molecular Devices) [39].

Real-time quantitative reverse transcription–polymerase chain reaction (RT-PCR)

Gene expression of NADPH oxidase subunits (NOX2, NOX4, p22phox, and p47phox), and reference genes cyclophilin and glyceraldeyde-3-phosphate dehydrogenase (GAPDH) was analysed by RT-PCR according to a previously described method [40, 41].

Total RNA was extracted from soleus muscles with TRIzol Reagent (Invitrogen Life Technologies, Carlsbad, CA, USA) and treated with DNase I (Invitrogen Life Technologies). One microgram of RNA was reverse transcribed using High Capacity cDNA Reverse Transcription Kit, according to standard methods (Applied Biosystems, Foster City, CA, USA). Aliquots of cDNA were then submitted to real time PCR reaction using customized assay containing sense and antisense primers and Taqman (Applied Biosystems, Foster City, CA, USA) probe specific to each gene: NOX2 (Rn00576710_m1), NOX4 (Rn00585380_m1), $p22^{phox}$ (Rn00577357_m1), and $p47^{phox}$ (Rn00586945_m1). The amplification and analysis were performed using Step One Plus™ Real-Time PCR System (Applied Biosystems, Foster City, CA, USA). Expression data were normalized to reference gene expressions: cyclophilin (Rn00690933_m1), and GAPDH (Rn01775763_g1). Reactions were performed in triplicate and expression levels calculated using the CT comparative method ($2^{-\Delta\Delta CT}$) [42].

Statistical analysis

Data are expressed as mean±standard deviation. Comparisons between groups were performed by one-way ANOVA and Bonferroni post hoc test (comparisons of interest: Sham versus MI-C and MI-C versus MI-NAC). The Student's *t*-test was used to compare MI size. Significance level was set at 5%.

Results

Experimental groups and anatomical variables

Sham group rats (n=16) did not present any heart failure features. The frequency of heart failure features in MI-C and MI-NAC groups is shown in Table 1. Anatomical data are presented in Table 2. Soleus muscle weight (Sham 0.25±0.03; MI-C 0.23±0.04; MI-NAC 0.22±0.03 g; $p>0.05$) and soleus-to-BW ratio (Sham 0.49±0.06; MI-C 0.49±0.05; MI-NAC 0.48±0.07 mg/kg; $p>0.05$) did not differ between groups. Myocardial infarction size did not differ between MI-C (47.5±5.7%) and MI-NAC (47.2±8.6%) groups.

Echocardiograph evaluation

Before NAC administration, all echocardiographic variables were similar between MI-C and MI-NAC groups (data not shown). Cardiac structural and left ventricular function variables evaluated at the end of the experiment are shown in Tables 3 and 4, respectively.

Table 1. Frequency of heart failure features in the infarcted rats

	Frequency (%)	
	MI-C (n=16)	MI-NAC (n=16)
Tachypnea/labored respiration	62.5	50.0
Left atrial thrombi	12.5	18.8
Pleuropericardial effusion	75.0	50.0
Pulmonary congestion	75.0	56.3
Right ventricular hypertrophy	68.8	50.0

MI-C: infarcted rats without treatment; MI-NAC: infarcted rats treated with *N*-acetylcysteine.

Table 2. Anatomical data

	Sham (n=16)	MI-C (n=16)	MI-NAC (n=16)
BW (g)	506±49	461±55*	458±52
LVW (g)	0.90±0.10	0.89±0.10	0.89±0.09
RVW (g)	0.27±0.03	0.46±0.16*	0.42±0.17
Lung (g)	2.04±0.21	3.13±0.99*	2.75±0.82
LVW/BW (mg/g)	1.78±0.14	1.93±0.12*	1.96±0.21
RVW/BW (mg/g)	0.54±0.06	1.00±0.32*	0.93±0.36
Lung/BW (mg/g)	4.06±0.48	6.73±1.79*	6.07±1.84

MI-C: infarcted rats without treatment; MI-NAC: infarcted rats treated with *N*-acetylcysteine; BW: body weight; LVW: left ventricle weight; RVW: right ventricle weight. *$p<0.05$ vs. Sham; ANOVA and Bonferroni.

Table 3. Cardiac structure parameters

	Sham (n=16)	MI-C (n=16)	MI-NAC (n=16)
LVDD (mm)	8.89±0.58	11.15±1.51*	10.74±1.09
LVDD/BW (mm/kg)	16.61±1.78	22.35±2.48*	21.74±2.17
LVSD (mm)	4.60±0.54	8.88±1.54*	8.73±1.40
PWT (mm)	1.51±0.13	1.91±0.31*	1.78±0.42
AO (mm)	4.0±0.2	3.7±0.2*	3.8±0.2
LA (mm)	6.2±0.5	8.4±0.9*	8.1±1.1
LA/BW (mm/kg)	11.55±1.36	17.65±2.13*	17.28±2.67

MI-C: infarcted rats without treatment; MI-NAC: infarcted rats treated with *N*-acetylcysteine. LVDD and LVSD: LV diastolic and systolic diameters, respectively; BW: body weight; PWT: LV diastolic posterior wall thickness; AO: aorta diameter; LA: left atrium diameter. *p<0.05 vs. sham; ANOVA and Bonferroni.

Table 4. Left ventricular function data

	Sham (n=16)	MI-C (n=16)	MI-NAC (n=16)
HR (beats/min)	270±30	296±64	275±33
FS (%)	48.2±4,3	20.7±4.9*	19.1±5.9
ΔArea (%)	67.6±6.0	25.3±5.8*	28.7±6.0
PWSV (mm/s)	37.7±3.3	22.4±4.0*	20.8±4.7
E/A	1.45±0.14	5.45±2.44*	3.77±2.48#
EDT (ms)	50.0±4.9	37.1±10.6*	40.2±12.0
IVRT/R-R	57.7±10.1	68.8±11.8*	66.6±15.1

MI-C: infarcted rats without treatment; MI-NAC: infarcted rats treated with *N*-acetylcysteine. HR: heart rate; FS: endocardial fractional shortening; ΔArea: area fractional shortening; PWSV: posterior wall shortening velocity; E/A: early-to-late diastolic mitral inflow ratio; EDT: E-wave deceleration time; IVRT/R-R: isovolumetric relaxation time normalized to heart rate. *p<0.05 vs. sham; #p<0.05 vs. MI-C; ANOVA and Bonferroni.

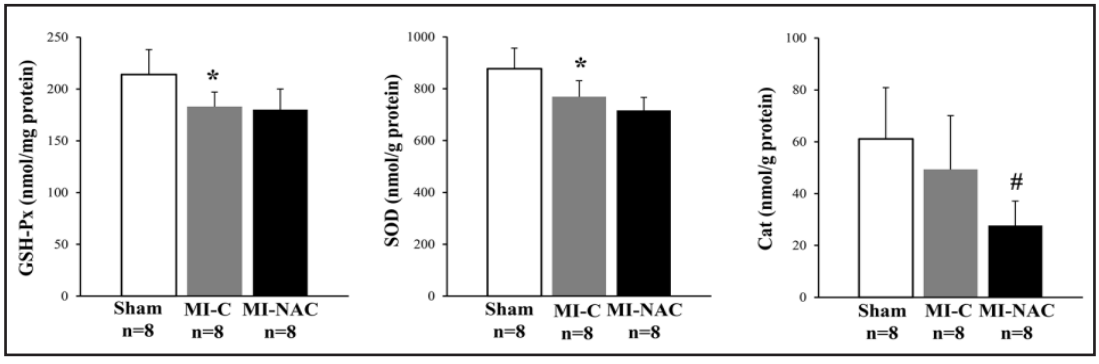

Fig. 1. Antioxidant enzymes activity in soleus muscle. GSH-Px: glutathione peroxidase; SOD: superoxide dismutase; Cat: catalase. Mean ± standard deviation; ANOVA and Bonferroni; *p<0.05 *vs.* Sham; #p<0.05 *vs.* MI-C.

Oxidative stress evaluation

Antioxidant enzymes activity. GSH-Px and SOD activity was reduced in MI-C than Sham and did not differ between MI-NAC and MI-C (GHS-Px: Sham 214±24; MI-C 183±14; MI-NAC 180±20 nmol/mg protein; p=0.005; SOD: Sham 877±80; MI-C 769±62; MI-NAC 716±51 nmol/g protein; p<0.001; Fig. 1). Catalase activity was similar in Sham and MI-C, and lower in MI-NAC than MI-C (Sham 61.1±19.8; MI-C 49.3±20.8; MI-NAC 27.7±9.4 nmol/g protein; p=0.003; Fig. 1).

Oxidative stress markers. Soleus muscle lipid hydroperoxide concentration did not differ between groups (Sham 248±13; MI-C 261±29; MI-NAC 249±25 nmol/g tissue; p=0.47; Fig. 2A). The 3-nitrotyrosine muscle concentration was similar between Sham and MI-C, and lower in MI-NAC than MI-C (Sham 2.89±0.80; MI-C 3.33±0.95; MI-NAC 2.1±0.96 nM/mg protein; p=0.039; Fig. 2B).

Considering systemic oxidative stress marker levels, MDA serum concentration was higher in MI-C than Sham and did not differ between MI-C and MI-NAC (Sham 0.98±0.22;

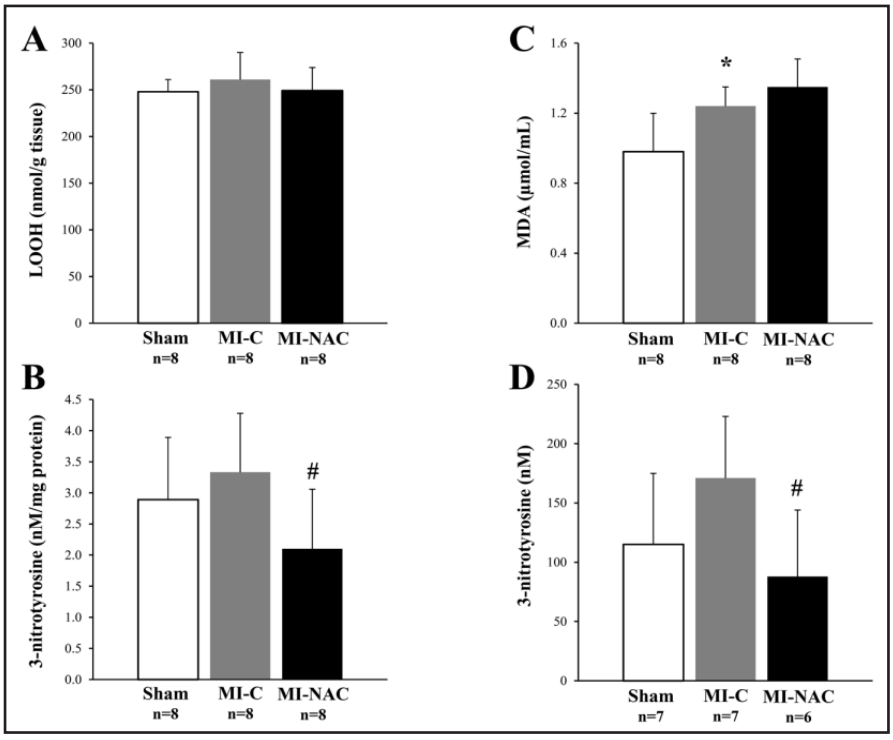

Fig. 2. Soleus muscle (*A* and *B*) and serum (*C* and *D*) oxidative stress markers concentration. LOOH: lipid hydroperoxide; MDA: malondialdehyde. Mean ± standard deviation; ANOVA and Bonferroni; **p*<0.05 *vs.* Sham; #*p*<0.05 *vs.* MI-C.

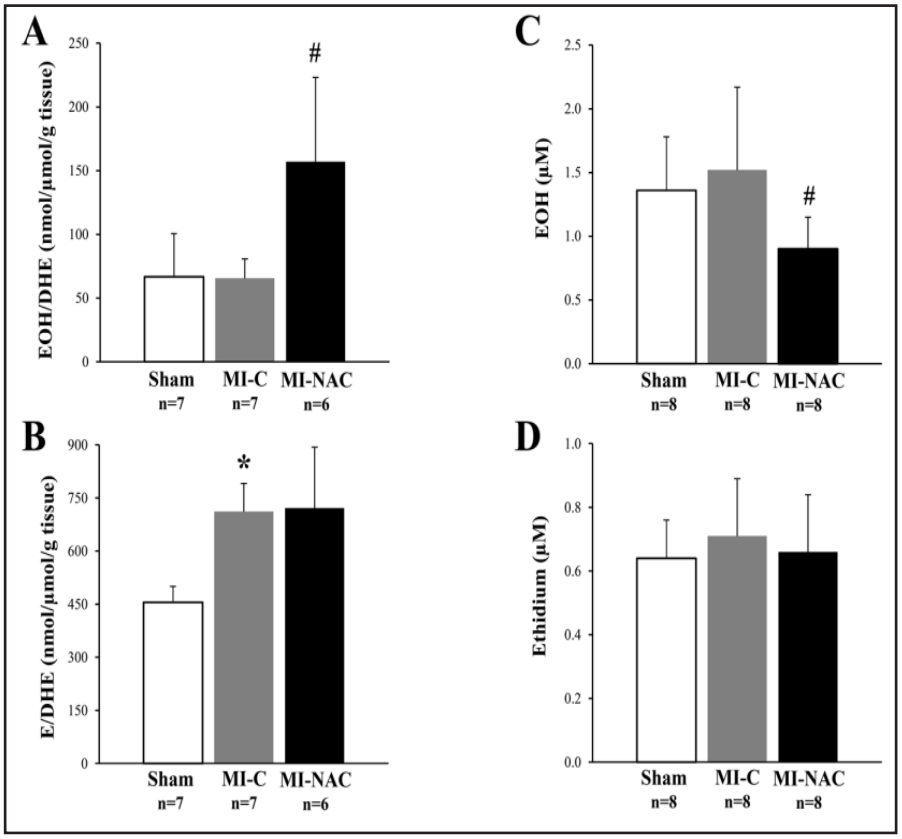

Fig. 3. Quantification of two dihydroethidium (DHE) oxidation-derived fluorescent compounds by HPLC: 2-hydroxyethidium (EOH), and ethidium (E). *A and B*: Total reactive oxygen species generation in soleus muscle. *C and D*: NADPH oxidase enzyme activity in soleus muscle. Mean ± standard deviation; ANOVA and Bonferroni; **p*<0.05 *vs.* Sham; #*p*<0.05 *vs.* MI-C.

MI-C 1.24±0.11; MI-NAC 1.35±0.16 µmol/mL; $p<0.001$; Fig. 2C). The 3-nitrotyrosine serum concentration was similar in Sham and MI-C, and lower in MI-NAC than MI-C (Sham 115±60; MI-C 171±52; MI-NAC 88±56 nM; $p<0.045$; Fig. 2D).

Table 5. Gene expression of NADPH oxidase enzyme subunits

	Sham (n=8)	MI-C (n=8)	MI-NAC (n=8)
NOX2	1.00±0.53	0.85±0.26	0.60±0.26
NOX4	1.00±0.30	1.09±0.12	0.79±0.17#
$p22^{phox}$	1.00±0.21	1.09±0.13	0.79±0.19#
$p47^{phox}$	1.00±0.13	0.83±0.08*	0.81±0.20

MI-C: infarcted rats without treatment; MI-NAC: infarcted rats treated with *N*-acetylcysteine. *p<0.05 vs. Sham; #p<0.05 vs. MI-C; ANOVA and Bonferroni.

ROS generation. EOH/DHE ratio did not differ between Sham and MI-C, and was higher in MI-NAC than MI-C (Sham 67±34; MI-C 66±15; MI-NAC 157±66 nmol/µmol/g tissue; p=0.001; Fig. 3A). Ethidium/DHE ratio was higher in MI-C than Sham and similar in MI-NAC and MI-C (Sham 455±45; MI-C 711±80; MI-NAC 721±172 nmol/µmol/g tissue; p<0.001; Fig. 3B).

NADPH oxidase activity. EOH was similar in Sham and MI-C, and lower in MI-NAC than MI-C (Sham 1.36±0.42; MI-C 1.52±0.65; MI-NAC 0.90±0.25 µM; p=0.041; Fig. 3C). Ethidium was similar in all groups (Sham 0.64±0.12; MI-C 0.71±0.18; MI-NAC 0.66±0.18 µM; p>0.05; Fig. 3D). Amplex Red® assay showed similar H_2O_2 production in all groups (Sham 100±41; MI-C 146±59; MI-NAC 130±61 %; p>0.05).

Gene expression

NADPH oxidase complex subunit mRNA expressions are presented in Table 5. NOX2 expression did not differ between groups. NOX4 e p22phox gene expression was similar between Sham and MI-C, and lower in MI-NAC than in MI-C. In addition, p47phox expression was lower in MI-C than in Sham group, and similar between MI-C and MI-NAC groups.

Discussion

In this study we confirmed that oxidative stress is increased in skeletal muscle of heart failure rats and showed that oxidative stress is not related to increased NADPH oxidase activity. Additionally, we assessed for the first time the influence of the antioxidant *N*-acetylcysteine on oxidative stress markers.

Experimental myocardial infarction models have been widely used for inducing heart failure. However, only rats with moderate to large myocardial infarction develop heart failure [24]. In this study, rats from MI-C and MI-NAC groups had similar infarct sizes, approximately 48%, which is considered large. Heart failure diagnosis was based on observation of clinical and pathologic features [24, 25] and confirmed by the greater right ventricle and lung weights in MI-C than Sham group. *N*-acetylcysteine did not modify these variables.

Before *N*-acetylcysteine treatment, echocardiographic analysis showed that MI-C and MI-NAC groups had a similar degree of cardiac injury (data not shown). After two months of treatment, echocardiographic evaluation showed MI-C rats with dilated left cardiac chambers combined with systolic and diastolic left ventricular dysfunction compared to Sham animals. Diastolic dysfunction was severe in MI-C group, with a restrictive pattern characterized by an increased E/A ratio [24]. Late treatment with NAC did not attenuate structural cardiac changes or systolic ventricular dysfunction, but slightly improved diastolic function, as shown by the lower E/A ratio in MI-NAC. Recent studies have shown that NAC administration initiated 24 hours [43] or two months [23] after MI improves fractional shortening and attenuates cardiac remodelling. As treatment in our study was started four months after MI, it is probable that rats had already presented advanced degrees of left cardiac chambers dilation and ventricular systolic dysfunction, preventing a reverse remodelling process.

Concerning to redox status in skeletal muscle, GSH-Px and SOD enzymes activity was reduced in infarcted groups. Decreased antioxidant enzymes activity in skeletal muscle has already been demonstrated in clinical and experimental studies [5, 14]. The deleterious

effects of oxygen and nitrogen reactive species can be controlled by a complex endogenous antioxidant system that includes antioxidant enzymes GSH-Px, SOD, and catalase. SOD catalyses superoxide dismutation to H_2O_2 and O_2 in the presence of H^+ ion. Furthermore, H_2O_2 generated by SOD activity generates water and oxygen by catalase. However, GSH-Px activity depends on glutathione concentration. Glutathione can be found in reduced (GSH) or oxidized (GSSG) forms. Its antioxidant property comes from the ability to react with H_2O_2 and organic peroxides by GSH-Px activity with consequent GSH to GSSG oxidation. NAC treatment reduced catalase activity and did not restore SOD or GSH-Px activity. A recent study showed that NAC administration restores total glutathione levels and reduces H_2O_2 and lipid hydroperoxide concentrations in left ventricle from infarcted rats [23]. However, no studies evaluating the influence of NAC treatment on skeletal muscle from heart failure rats were found.

We next evaluated NADPH oxidase complex, an important ROS source. The NOX2 catalytic subunit forms a complex with $p22^{phox}$ which depends on $p47^{phox}$ and $p67^{phox}$ cytosolic regulatory subunits linkage being activated [17]. Although we observed reduced $p47^{phox}$ gene expression in MI-C, it is possible that $p47^{phox}$ protein levels (not evaluated in this study) were preserved as was NADPH oxidase activity. Conversely, even though NOX4 interacts with transmembrane protein $p22^{phox}$, it differs from other isoforms because it is constitutively active and independent of regulatory or activator cytosolic proteins [17]. In this study, gene expression of NOX4 and $p22^{phox}$ subunits was not altered in MI-C, which is in accordance with the unchanged NADPH oxidase activity. Information on the role of NADPH oxidase in heart failure-associated skeletal myopathy is scarce. We have identified only one study by Ohta et al. [20], who differently from us, observed increased NADPH oxidase activity in mice skeletal muscle one month after inducing MI. However, as in other studies [44], the authors analysed NADPH oxidase activity with a chemiluminescent assay using lucigenin which can be reduced by superoxide anion. In our study, we assayed NADPH oxidase activity using DHE, a molecule which is oxidized by superoxide anion. Thus, our results may have diverged from the Ohta et al. [20] due to the different animal model and NADPH oxidase activity analytical technique.

NAC administration decreased NOX4 and $p22^{phox}$ and did not restore $p47^{phox}$ gene expression. Additionally, NADPH oxidase activity was lower in MI-NAC than MI-C. NOX2 activity generates superoxide as a primary product, and hydrogen peroxide (H_2O_2) as a secondary product derived from superoxide dismutation [17]. Recent studies have shown that NOX4 can directly produce H_2O_2 [39]. Therefore, even though NOX2 gene expression was unchanged in our study, the reduced $p22^{phox}$gene expression was associated to decreased superoxide production. Conversely, decreased H_2O_2 generation was also expected because superoxide generation was lower, but this did not occur probably because NAC did not restore SOD activity. Also, reduced NOX4 and $p22^{phox}$ gene expression might have led to lower H_2O_2 production, which unexpectedly did not happen. Additional studies evaluating protein levels of NADPH oxidase enzyme subunits are needed to confirm our data on gene expression.

The oxidative stress markers malondialdehyde and nitrotyrosine were also analysed. We observed that NAC acted differentially on MDA and nitrotyrosine. Several proteins have sulfhydryl groups whose oxidation may lead to protein function loss. Glutathione is able to protect and also regenerate these sulfhydryl groups against ROS attack [45]. Regarding lipid peroxidation, direct glutathione action is only slightly efficient as it is found in aqueous cells compartments. Glutathione depends on GSH-Px activity to remove lipoperoxidation-derived products [46]. In our study, GSH-Px was not restored by NAC treatment and may have contributed to maintaining the elevated MDA serum concentration.

Total ROS production was evaluated in soleus muscle. We identified a higher ethidium/DHE ratio in MI-C compared to Sham and no difference between MI-NAC and MI-C. Besides the origin of the ethidium product being not completely clarified, Fernandes et al. [37] suggested that complex pathways, including heme levels and peroxidase activity, may contribute to its formation. However, as we did not analyse these pathways, the association

between heme levels and peroxidase activity and ethidium generation is a hypothesis that needs further confirmation. Also, EOH/DHE ratio was not statistically different between Sham and MI-C, but was surprisingly higher in MI-NAC than MI-C. Evidence has shown that increasing glutathione levels through NAC protects against oxidative stress in several diseases, including heart failure. However, recent studies have documented that, contrary to the common belief that NAC functions solely as an antioxidant, excess glutathione from NAC treatment culminates in reductive stress with pro-oxidative consequences in mitochondria and augmented ROS levels [47], which may have occurred in our experimental model. Although it has been documented in other studies, the NAC-induced ROS elevation should be further investigated in this experimental model, and it can be considered a limitation of the present study. Furthermore, other antioxidant small molecules should be investigated to verify their efficacy on modulating oxidative stress.

Clinical Perspectives

Heart failure-induced skeletal muscle changes are a high prevalent clinical condition, which is associated with important limitation of functional capacity. Nowadays, there is no specific pharmacologic therapy for skeletal muscle alterations. Therefore, identifying physiopathological mechanisms involved in these alterations is important to develop strategies to prevent and treat muscle deterioration. In this study, we showed that oxidative stress is increased in skeletal muscle of heart failure rats, but is not related to increased NADPH oxidase activity. We also showed that the antioxidant *N*-acetylcysteine acts differentially on oxidative stress markers. The results suggest that *N*-acetylcysteine can have a role in modulating skeletal muscle oxidative stress during heart failure.

In conclusion, in this study we confirm that oxidative stress is increased in slow-twitch soleus muscle of heart failure rats, despite unchanged NADPH oxidase activity. *N*-acetylcysteine is partially effective in reducing oxidative stress, as it decreases NADPH oxidase activity and 3-nitrotyrosine levels.

Acknowledgments

We are grateful to Jose Carlos Georgette, Mario Batista Bruno, Maria Bertolini, and Victor Debbas for technical assistance and Colin Edward Knaggs for English editing. Financial support: Fundação de Amparo à Pesquisa do Estado de São Paulo (FAPESP; proc. 2010/50461-6 and 2007/59500-1), Conselho Nacional de Desenvolvimento Científico e Tecnológico (CNPq; proc. 306857/2012-0 and 306.845/2012-1), Pro-Reitoria de Pesquisa da Universidade Estadual Paulista (PROPe/UNESP), and Fundacao para o Desenvolvimento da UNESP (Fundunesp). The funders had no role in study design, data collection and analysis, decision to publish, or preparation of the manuscript.

Disclosure Statement

There is no conflict of interest to disclosure.

References

1 Harrington D, Anker SD, Chua TP, Webb-Peploe KM, Ponikowski PP, Poole-Wilson PA, Coats AJS: Skeletal muscle function and its relation to exercise tolerance in chronic heart failure. J Am Coll Cardiol 1997;30:1758-1764.

2 Strassburg S, Springer J, Anker SD: Muscle wasting in cardiac cachexia. Intern J Biochem Cell Biol 2005;37:1938-1947.

3 von Haehling S, Steinbeck L, Doehner W, Springer J, Anker SD: Muscle wasting in heart failure: an overview. Int J Biochem Cell Biol 2013;45:2257-2265.

4 Mancini DM, Walter G, Reichek N, Lenkinski R, McCully KK, Mulle JL, Wilson JR: Contribution of skeletal muscle atrophy to exercise intolerance and altered muscle metabolism in heart failure. Circulation 1992;85:1364-1373.

5 Moreira JB, Bechara LR, Bozi LH, Jannig PR, Monteiro AW, Dourado PM, Wisløff U, Brum PC: High-versus moderate-intensity aerobic exercise training effects on skeletal muscle of infarcted rats. J Appl Physiol 2013;114:1029-1041.
6 Damatto RL, Martinez PF, Lima AR, Cezar MD, Campos DH, Oliveira Jr SA, Guizoni DM, Bonomo C, Nakatani BT, Dal Pai-Silva M, Carvalho RF, Okoshi K, Okoshi MP: Heart failure-induced skeletal myopathy in spontaneously hypertensive rats. Int J Cardiol 2013;167:698-703.
7 Martinez PF, Okoshi K, Zornoff LAM, Carvalho RF, Oliveira Jr SA, Lima AR, Campos DH, Damatto RL, Nogueira CR, Dal Pai-Silva M, Okoshi MP: Chronic heart failure-induced skeletal muscle atrophy, necrosis, and myogenic regulatory factors changes. Med Sci Monit 2010;16:374-383.
8 Carvalho RF, Dariolli R, Justulin Jr LA, Sugizaki MM, Okoshi MP, Cicogna AC, Felisbino SL, Dal Pai-Silva M: Heart failure alters matrix metalloproteinase gene expression and activity in rat skeletal muscle. Int J Exp Pathol 2006;87:437-443.
9 Lima AR, Martinez PF, Okoshi K, Guizoni DM, Zornoff LAM, Campos DH, Oliveira Jr SA, Bonomo C, Dal Pai-Silva M, Okoshi MP: Myostatin and follistatin expression in skeletal muscles of rats with chronic heart failure. Int J Exp Path 2010;91:54-62.
10 Santos DP, Okoshi K, Moreira VO, Seiva FRF, Almeida FLA, Padovani CR, Carvalho RF, Okoshi MP, Cicogna AC, Castro AVB, Dal Pai-Silva M: Growth hormone attenuates skeletal muscle changes in experimental chronic heart failure. Growth Horm IGF Res 2010;20:149-155.
11 Carvalho RF, Cicogna AC, Campos GER, Assis JMF, Padovani CR, Okoshi MP, Dal Pai-Silva M: Myosin heavy chain expression and atrophy in rat skeletal muscle during transition from cardiac hypertrophy to heart failure. Int J Exp Path 2003;84:201-206.
12 Octavia Y, Brunner-La Rocca HP, Moens AL: NADPH oxidase-dependent oxidative stress in the failing heart: From pathogenic roles to therapeutic approach. Free Radic Biol Med 2012;52:291-297.
13 Madamanchi NR, Runge MS: Redox signaling in cardiovascular health and disease. Free Rad Biol Med 2013;61:473-501.
14 Linke A, Adams V, Schulze PC, Erbs S, Gielen S, Fiehn E, Mobius-Winkler S, Schubert A, Schuler G, Hambrecht R: Antioxidative effects of exercise training in patients with chronic heart failure: increase in radical scavenger enzyme activity in skeletal muscle. Circulation 2005;111:1763-1770.
15 Tsutsui H, Ide T, Hayashidani S, Suematsu N, Shiomi T, Wen J, Nakamura K, Ichikawa K, Utsumi H, Takeshita A: Enhanced generation of reactive oxygen species in the limb skeletal muscles from a murine infarct model of heart failure. Circulation 2001;104:134-136.
16 Cunha TF, Bacurau AVN, Moreira JBN, Paixão NA, Campos JC, Ferreira JCB, Leal ML, Negrão CE, Moriscot AS, Wisløff U, Brum PC: Exercise training prevents oxidative stress and ubiquitin-proteasome system overactivity and reverse skeletal muscle atrophy in heart failure. PLoS ONE 2012:e41701.
17 Bedard K, Krause K-H: The NOX family of ROS-generating NADPH oxidases: physiology and pathophysiology. Physiol Rev 2007;87:245-313.
18 Sullivan-Gunn M, Campbell-O'Sullivan S, Tisdale MJ, Lewandowski PA: Decreased NADPH oxidase expression and antioxidant activity in cachectic skeletal muscle. J Cachexia Sarcopenia Muscle 2011;2:181-188.
19 Mofarrahi M, Brandes RP, Gorlach A, Hanze J, Terada LS, Quinn MT, Mayaki D, Petrof B, Hussain SN: Regulation of proliferation of skeletal muscle precursor cells by NADPH oxidase. Antioxid Redox Signal 2008;10:559-574.
20 Ohta Y, Kinugawa T, Matsushima S, Ono T, Sobirin MA, Inoue N, Yokota T, Hirabayashi K, Tsutsui H: Oxidative stress impairs insulin signal in skeletal muscle and causes insulin resistance in postinfarct heart failure. Am J Physiol Heart Circ Physiol 2011;300:H1637-H1644.
21 Fratelli M, Goodwin LO, Orom UA, Lombardi S, Tonelli R, Mengozzi M, Ghezzi P: Gene expression profiling reveals a signaling role of glutathione in redox regulation. Proc Natl Acad Sci USA 2005;102:13998-14003.
22 Wang T, Mao X, Li H, Qiao S, Xu A, Wang J, Lei S, Liu Z, Ng KFJ, Wong GT, Vanhoutte PM, Irwin MG, Xia Z: N-Acetylcysteine and allopurionl up-regulated the Jak/STAT3 and PI3K/Akt pathways via adiponectin and attenuated myocardial postischemic injury in diabetes. Free Rad Biol Med 2013;63:291-303.
23 Adamy C, Mulder P, Khouzami L, Andrieu-Abadie N, Defer N, Candiani G, Pavoine C, Caramelle P, Souktani R, Le Corvoisier P, Perier M, Kirsch M, Damy T, Berdeaux A, Levade T, Thuillez C, Hittinger L, Pecker F: Neutral sphingomyelinase inhibition participates to the benefits of N-acetylcysteine treatment in post-myocardial infarction failing heart rats. J Mol Cell Cardiol 2007;43:344-353.
24 Martinez PF, Okoshi K, Zornoff LA, Oliveira Jr SA, Campos DH, Lima AR, Damatto RL, Cezar MD, Bonomo C, Guizoni DM, Padovani CR, Cicogna AC, Okoshi MP: Echocardiographic detection of congestive heart failure in postinfarction rats. J Appl Physiol 2011;111:543-551.

25 Cicogna AC, Robinson KG, Conrad CH, Singh K, Squire R, Okoshi MP, Bing OHL: Direct effects of colchicine on myocardial function. Studies in hypertrophied and failing spontaneously hypertensive rats. Hypertension 1999;33:60-65.
26 Sugizaki MM, Carvalho RF, Aragon FF, Padovani CR, Okoshi K, Okoshi MP, Zanati SG, Dal Pai-Silva M, Novelli EL, Cicogna AC: Myocardial dysfunction induced by food restriction is related to morphological damage in normotensive middle-aged rats. J Biomed Sci 2005;12:641-649.
27 Oliveira Jr SA, Dal Pai Silva M, Martinez PF, Lima-Leopoldo AP, Campos DH, Leopoldo AS, Okoshi MP, Okoshi K, Padovani CR, Cicogna AC: Diet-induced obesity causes metabolic, endocrine and cardiac alterations in spontaneously hypertensive rats. Med Sci Monit 2010;16:BR367-BR373.
28 Nascimento AF, Luvizotto RA, Leopoldo AS, Lima-Leopoldo AP, Seiva FR, Justulin Jr LA, Dal Pai-Silva M, Okoshi K, Wang XD, Cicogna AC: Long-term high-fat diet-induced obesity decreases the cardiac leptin receptor without apparent lipotoxicity. Life Sci 2011;88:1031-1038.
29 Oliveira-Jr AS, Martinez PF, Guizoni DM, Campos DH, Fernandes T, Oliveira EM, Okoshi MP, Okoshi K, Padovani CR, Cicogna AC: AT1 receptor blockade attenuates insulin resistance and myocardial remodeling in rats with diet-induced obesity. PLoS ONE 2014:e86447.
30 Minicucci MF, Azevedo PS, Martinez PF, Lima AR, Bonomo C, Guizoni DM, Polegato BF, Okoshi MP, Okoshi K, Matsubara BB, Paiva SAR, Zornoff LA: Critical infarct size to induce ventricular remodeling, cardiac dysfunction and heart failure in rats. Int J Cardiol 2011;151:242-243.
31 Diniz YS, Rocha KKHR, Souza GA, Galhardi CM, Ebaid GMX, Rodrigues HG, Novelli Filho JLVB, Cicogna AC, Novelli ELB: Effects of N-acetylcysteine on sucrose-rich diet-induced hyperglycaemia, dyslipidemia and oxidative stress in rats. Eur J Pharmacol 2006;543:151–157.
32 Nakamura W, Hojoda S, Hayashi K: Purification and properties of rat liver glutathione peroxidase. Biochem Biophys Acta 1974;358:251-261.
33 Ewing JF, Janero DR: Microplate superoxide dismutase assay employing a nonenzymatic superoxide generator. Anal Biochem 1995;232:243-248.
34 Aebi H: Methods of enzymatic analysis. 2nd ed. Verloy Chemia Weinheim New York, 1974.
35 Jiang ZY, Woollard AC, Wolff SP: Lipid hydroperoxide measurement by oxidation of Fe2+ in the presence of xylenol orange. Comparison with the TBA assay and an iodometric method. Lipids 1991;26:853-856.
36 Li L, Chen C-YO, Aldini G, Johnson EJ, Rasmussen H, Yoshida Y, Niki E, Blumberg JB, Russell RM, Yeum K-J: Supplementation with lutein or lutein plus green tea extracts does not change oxidative stress in adequately nourished older adults. J Nutr Biochem 2010;21:544-549.
37 Fernandes DC, Wosniak J, Pescatore LA, Bertoline MA, Liberman M, Laurindo FRM, Santos CXC: Analysis of DHE-derived oxidation products by HPLC in the assessment of superoxide production and NADPH oxidase activity in vascular systems. Am J Phyiol Cell Physiol 2007;292:C413-C422.
38 Laurindo FRM, Fernandes DC, Santos CXC: Assessment of superoxide production and NADPH oxidase activity by HPLC analysis of dihydroethidium oxidation products. Methods Enzymol 2008;441:237-260.
39 Takac I, Schroder K, Zhang L, Lardy B, Anilkumar N, Lambeth JD, Shah AM, Morel F, Brandes RP: The E-loop is involved in hydrogen peroxide formation by the NADPH oxidase Nox4. J Biol Chem 2011;286:13304-13313.
40 Cezar MD, Damatto RL, Martinez PF, Lima AR, Campos DH, Rosa CM, Guizoni DM, Bonomo C, Cicogna AC, Gimenes R, Pagan LU, Okoshi MP, Okoshi K: Aldosterone blockade reduces mortality without changing cardiac remodeling in spontaneously hypertensive rats. Cell Physiol Biochem 2013;32:1275-1287.
41 Rosa CM, Xavier NP, Campos DH, Fernandes AA, Cezar MD, Martinez PF, Cicogna AC, Gimenes C, Gimenes R, Okoshi MP, Okoshi K: Diabetes mellitus activated fetal gene program and intensifies cardiac remodeling and oxidative stress in aged spontaneously hypertensive rats. Cardiovasc Diabetol 2013;12:152.
42 Livak KJ, Schmittgen TD: Analysis of relative gene exression data using real-time quantitative PCR and the 2-DDCT method. Methods 2001;25:402-408.
43 Lee TM, Lai PY, Chang NC: Effect of N-acetylcysteine on sympathetic hyperinnervation in post-infarcted rat hearts. Cardiovasc Res 2010;85:137-146.
44 Cheng S-E, Lee I-T, Lin C-C, Wu W-L, Hsiao L-D, Yang C-M: ATP mediates NADPH oxidase/ROS generation and COX-2/PGE2 expression in A549 cells: role of P2 receptor-dependent STAT3 activation. PLoS ONE 2013;8:e54125.
45 Lushchak VI: Glutathione homeostasis and functions: potential targets for medical interventions. J Amino Acids 2012;2012:736837.
46 Shan XQ, Aw TY, Jones DP: Glutathione-dependent protection against oxidative injury. Pharmacol Ther 1990;47:61-71.
47 Zhang H, Limphong P, Pieper J, Liu Q, Rodesch CK, Christians E, Benjamin IJ: Glutathione-dependent reductive stress triggers mitochondrial oxidation and cytotoxicity. FASEB J 2012;26:1442-1451.